



OPEN ACCESS

EDITED BY

Hasem Habelhah,
The University of Iowa, United States

REVIEWED BY

Yumei Fan,
Hebei Normal University, China
Bernard Haendler,
Bayer, Germany

*CORRESPONDENCE

Paul Dent
paul.dent@vcuhealth.org

SPECIALTY SECTION

This article was submitted to
Cancer Molecular Targets
and Therapeutics,
a section of the journal
Frontiers in Oncology

RECEIVED 15 September 2022

ACCEPTED 14 October 2022

PUBLISHED 03 November 2022

CITATION

Booth L, Roberts JL, West C and
Dent P (2022) GZ17-6.02 kills prostate
cancer cells *in vitro* and *in vivo*.
Front. Oncol. 12:1045459.
doi: 10.3389/fonc.2022.1045459

COPYRIGHT

© 2022 Booth, Roberts, West and Dent.
This is an open-access article
distributed under the terms of the
[Creative Commons Attribution License
\(CC BY\)](https://creativecommons.org/licenses/by/4.0/). The use, distribution or
reproduction in other forums is
permitted, provided the original
author(s) and the copyright owner(s)
are credited and that the original
publication in this journal is cited, in
accordance with accepted academic
practice. No use, distribution or
reproduction is permitted which does
not comply with these terms.

GZ17-6.02 kills prostate cancer cells *in vitro* and *in vivo*

Laurence Booth¹, Jane L. Roberts¹, Cameron West²
and Paul Dent^{1*}

¹Department of Biochemistry and Molecular Biology, Virginia Commonwealth University, Richmond, VA, United States, ²Genzada Pharmaceuticals, Sterling, KS, United States

GZ17-6.02 is undergoing clinical evaluation in solid tumors and lymphoma. We defined the biology of GZ17-6.02 in prostate cancer cells and determined whether it interacted with the PARP1 inhibitor olaparib to enhance tumor cell killing. GZ17-6.02 interacted in a greater than additive fashion with olaparib to kill prostate cancer cells, regardless of androgen receptor expression or loss of PTEN function. Mechanistically, GZ17-6.02 initially caused peri-nuclear activation of ataxia-telangiectasia mutated (ATM) that was followed after several hours by activation of nuclear ATM, and which at this time point was associated with increased levels of DNA damage. Directly downstream of ATM, GZ17-6.02 and olaparib cooperated to activate the AMP-dependent protein kinase (AMPK) which then activated the kinase ULK1, resulting in autophagosome formation that was followed by autophagic flux. Knock down of ATM, AMPK α or the autophagy-regulatory proteins Beclin1 or ATG5 significantly reduced tumor cell killing. GZ17-6.02 and olaparib cooperated to activate protein kinase R which phosphorylated and inactivated eIF2 α , i.e., enhanced endoplasmic reticulum (ER) stress signaling. Knock down of eIF2 α also significantly reduced autophagosome formation and tumor cell killing. We conclude that GZ17-6.02 and olaparib interact to kill prostate cancer cells *in vitro* by increasing autophagy and by enhancing ER stress signaling. *In vivo*, GZ17-6.02 as a single agent profoundly reduced tumor growth and significantly prolonged animal survival. GZ17-6.02 interacted with olaparib to further suppress the growth of LNCaP tumors without ultimately enhancing animal survival. Our data support the consideration of GZ17-6.02 as a possible therapeutic agent in patients with AR+ prostate cancer.

KEYWORDS

GZ17-6.02, olaparib, PARP1, autophagy, ER stress, ATM

Abbreviations: ER, endoplasmic reticulum; AMPK, AMP-dependent protein kinase; mTOR, mammalian target of rapamycin; JAK, Janus kinase; STAT, Signal Transducers and Activators of Transcription; MAPK, mitogen activated protein kinase; CMV, empty vector plasmid; si, small interfering; SCR, scrambled; VEH, vehicle; 602, GZ17-6.02; Olap, olaparib; ER stress, GZ17-6.02, olaparib.

Introduction

GZ17-6.02 has three components: curcumin, harmine and isovanillin and is presently undergoing phase I safety evaluation in cancer patients with solid tumors and lymphoma (NCT03775525) (1–6). Over the past two years we have published data demonstrating that GZ17-6.02 kills a wide range of tumor cell types, including ER+ breast, colorectal, pancreatic, hepatic, biliary, NSCLC, cutaneous melanoma, sarcoma and actinic keratoses (1–6).

Our prior data using GZ17-6.02 demonstrated that it activated a DNA damage (ATM) and metabolism regulatory (AMPK) pathway, which resulted in enhanced autophagosome formation that was followed by autolysosome formation (autophagic flux). GZ17-6.02 activated PKR-like endoplasmic reticulum kinase (PERK) and increased the phosphorylation (inactivation) at serine 51 of eIF2 α , with ER stress signaling facilitating the autophagy response. The mechanisms of cell killing were multi-faceted requiring autophagy, ER stress signaling and death receptor signaling (1–6).

Prostate cancer, after cutaneous melanoma, is a major cause of cancer in US males (7). Successful treatment of the disease localized to the prostate utilizes surgery, brachytherapy, external beam radiotherapy and therapeutic interventions including anti-androgens and cytotoxic drugs such as Taxanes (8, 9). Non-organ-confined prostate cancer is usually treated first by androgen deprivation therapy (surgical or chemical castration) and then by AR signaling inhibitors. Treatment with Taxanes is used once resistance to full androgen blockade has been observed. In patients with disease localized in the prostate, their 5-year survival nears 100%, and even in patients who present with disseminated disease, a third will survive for at least 5 years. The PARP1 inhibitors olaparib and rucaparib are FDA approved for prostate cancer patients who present with advanced castration-resistant disease with homologous recombination repair deficits. For olaparib, recent clinical data strongly argues that the tumors of patients who have loss of function in BRCA1 and/or BRCA2 are most responsive to PARP1 inhibitors (10). The prostate cancer cell lines DU145, PC3 and LNCaP are commonly used for *in vitro* studies of the disease; DU145 and LNCaP have mutations in BRCA1 and BRCA2 whereas PC3 does not. The present studies were designed to investigate the biology of GZ17-6.02 in prostate cancer cells, and to define its interaction with the FDA-approved Poly ADP-ribosyl Polymerase 1 (PARP1) therapeutic olaparib.

Materials and methods

Materials

The LNCaP, PC3 and DU145 cell lines were obtained from the ATCC (Bethesda, MD). Olaparib was purchased from Selleckchem (Houston, TX). All Materials were obtained as

described in the references (1–6). Trypsin-EDTA, DMEM, RPMI, penicillin-streptomycin were purchased from GIBCOBRL (GIBCOBRL Life Technologies, Grand Island, NY). Other reagents and performance of experimental procedures were as described (1–6). Antibodies were purchased from Cell Signaling Technology (Danvers, MA); Abgent (San Diego, CA); Novus Biologicals (Centennial, CO); Abcam (Cambridge, UK); and Santa Cruz Biotechnology (Dallas, TX). Cell Signalling antibodies: ATM (D2E2) Rabbit mAb #2873; Phospho-ATM (Ser1981) (D25E5) Rabbit mAb #13050; AMPK α #2532; Phospho-AMPK α (Thr172) (D4D6D) Rabbit mAb #50081; mTOR #2972; Phospho-mTOR (Ser2448) #2971; Phospho-mTOR (Ser2481) #2974; ULK1 (R600) #4773; Phospho-ULK1 (Ser317) #37762; Phospho-ULK1 (Ser757) #6888; eIF2 α #9722; Phospho-eIF2 α (Ser51) #9721; PERK (D11A8) Rabbit mAb #5683; Phospho-PERK (Thr980) (16F8) Rabbit mAb #3179; AKT Antibody #9172; Phospho-AKT (Thr308) (244F9) Rabbit mAb #4056; STAT3 (124H6) Mouse mAb #9139; Phospho-STAT3 (Tyr705) Antibody #9131; STAT5 (D2O6Y) Rabbit mAb #94205; Phospho-STAT5 (Tyr694) #9351; Beclin-1 #3738; ATG5 (D5F5U) Rabbit mAb #12994; ATG13 (D4P1K) Rabbit mAb #13273; Phospho-ATG13 (Ser355) (E4D3T) Rabbit mAb #46329; GRP78/BiP #3183; CHOP (L63F7) Mouse mAb #2895 PPI α Antibody #2582; NF κ B p65 (L8F6) Mouse mAb #6956; Phospho-NF κ B p65 (Ser536) (93H1) Rabbit mAb #3033; Src (36D10) Rabbit mAb #2109; Phospho-Src Family (Tyr416) (E6G4R) Rabbit mAb #59548; Phospho-Src (Tyr527) Antibody #2015; c-MET (25H2) Mouse mAb #3127; Phospho-MET (Tyr1234/1235) Antibody #3126; FAS (4C3) Mouse mAb #8023; FAS-L (D1N5E) Rabbit mAb #68405; JAK1/2 (6G4) Rabbit mAb #3344; Phospho-Jak1 (Tyr1034/1035)/Jak2 (Tyr1007/1008) (E9Y7V) Mouse mAb #66245; c-KIT (D13A2) XP[®] Rabbit mAb #3074; Phospho-c-KIT (Tyr719) Antibody #3391; HER/ ErbB Family Antibody Sampler Kit #8339; p70 S6 Kinase #9202; Phospho-p70 S6 Kinase (Thr389) #2904; PDGF Receptor beta #3164; Phospho-PDGF Receptor beta (Tyr754) (23B2) Rabbit mAb #2992; Phospho-p44/42 MAPK (Erk1/2) (Thr202/Tyr204) (20G11) Rabbit mAb #4376; Histone Deacetylase (HDAC) Antibody Sampler Kit #9928; HDAC7 (D4E1L) Rabbit mAb #33418; HDAC8 (E7F5K) Rabbit mAb #66042; HDAC11 (D5I8E) Rabbit mAb #58442; MHC Class II (LGII-612.14) Mouse mAb #68258; p38 MAPK #9212; Phospho-p38 MAPK (Thr180/Tyr182) (3D7) Rabbit mAb #9215; LATS1 (C66B5) Rabbit mAb #3477; Phospho-LATS1/2 (Ser909) #9157; Phospho-LATS1/2 (Thr1079) (D57D3) Rabbit mAb #8654; YAP (1A12) Mouse mAb #12395; Phospho-YAP (Ser127) (D9W2I) Rabbit mAb #13008; Phospho-YAP (Ser109) (E5I9G) Rabbit mAb #53749; Phospho-YAP (Ser397) (D1E7Y) Rabbit mAb #13619; TAZ (E8E9G) Rabbit mAb #83669 Phospho-TAZ (Ser89) (E1X9C) Rabbit mAb #59971; NEDD4 Antibody #2740; PTEN Antibody #9552; Estrogen Receptor α (D6R2W) Rabbit mAb #13258; Cyclin Antibody Sampler Kit

dissolved in DMSO making a 10 mM stock solution, stored in multiple 100 μ l vials. The final concentration of DMSO is never more than 0.1% (v/v). Cells were not cultured in reduced serum media.

Assessments of protein expression and protein phosphorylation

Multi-channel fluorescence HCS microscopes perform true in-cell western blotting. Three independent cultures derived from three thawed vials of cells of a tumor were sub-cultured into individual 96-well plates (~5,000 cells per well). Twenty-four hours after plating, the cells are transfected with a control plasmid or a control siRNA, or with an empty vector plasmid or with plasmids to express various proteins. After another 24 hours, the cells are ready for drug exposure(s). At various time-points after the initiation of drug exposure, cells are fixed in place using paraformaldehyde and using Triton X100 for permeabilization. Primary antibodies (1:500 dilution for all experiments) are used, and plates are incubated at 4°C overnight with gentle rocking. Cells are washed three times with PBS and then subsequently incubated with validated fluorescent-tagged secondary antibodies (1:1000) for 30 min. Cells are then washed an additional three times with PBS. The microscope determines the background fluorescence in the well and in parallel randomly determines the mean fluorescent intensity of 100 cells per well. The counting is independent of cell density. Of note for scientific rigor is that the operator does not personally manipulate the microscope to examine specific cells; the entire fluorescent accrual method is independent of the operator. For representative images of cells that are typical of this process, please see references 1 and 6 (1–6).

Detection of cell death by trypan blue assay

Cells were treated with vehicle control or with drugs alone or in combination for 24h. At the indicated time points cells were harvested by trypsinization and centrifugation. Cell pellets were resuspended in PBS and mixed with trypan blue agent. Viability was determined microscopically using a hemocytometer. Five hundred cells from randomly chosen fields were counted and the number of dead cells was counted and expressed as a percentage of the total number of cells counted (1–6).

Transfection of cells with siRNA or with plasmids

Cells were plated and 24h after plating, transfected. Plasmids to express FLIP-s, BCL-XL, dominant negative caspase 9,

activated AKT, activated STAT3, activated mTOR and activated MEK1 EE were used throughout the study (Addgene, Waltham, MA). Empty vector plasmid (CMV) was used as a control. For siRNA transfection, 10 nM of the annealed siRNA or the negative control (a “scrambled” sequence with no significant homology to any known gene sequences from mouse, rat or human cell lines) were used (1–6).

Assessments of autophagosome and autolysosome levels

Cells were transfected with a plasmid to express LC3-GFP-RFP (Addgene, Watertown MA). Twenty-four hs after transfection, cells are treated with vehicle control or the drugs alone or in combination. Cells were imaged and recorded at 60X magnification 4h and 8h after drug exposure and the mean number of [GFP+RFP+] and [RFP+] punctae per cell determined from >50 randomly selected cells per condition (1–6).

Comet assays

Drug-treated cells, in suspension, are mixed with low melting point agarose and spread onto a microscope glass slide. After lysis of cells with detergent at a high salt concentration, DNA unwinding and electrophoresis was carried out at neutral pH (7–8). Unwinding of the DNA and electrophoresis at neutral pH permits the detection of double strand breaks and cross links. Collins et al. published a visual scoring method that classifies comets from grades 0–4 (11–13). One hundred comets were scored, and each comet assigned a value of 0 to 4 according to its class, the mean total score for the sample gel will be between 0 and 4 “arbitrary units.”

Animal studies

Studies were performed according to the U.S. Department of Agriculture regulations under the VCU IACUC protocol AD20008. Male NRG mice supplied by the Massey Cancer Center Animal Core (~20 g) were injected with 1.0×10^6 male LNCaP cells into their rear flank (10 animals per treatment group). Tumors were permitted to form for 1 week with tumors at that time exhibiting a mean volume of approximately 50 mm³. Mice were treated by oral gavage once every day for 45 days with vehicle control, GZ17-6.02 (50 mg/kg), olaparib (10 mg/kg) or the drugs in combination. Before, during and after drug treatment tumors were calipered every ~3 days as indicated in the Figure and tumor volume was assessed up to 45 days later. Tumor volumes under each condition are plotted. Animals were humanely killed when the tumor volume reached approximately 2,000 mm³ due to ulceration. Animal survival was plotted on a Kaplan–Meier curve.

Animal body mass under all treatment conditions did not significantly change over the 45-day time course.

Data analysis

Comparison of the effects of various treatments was using one-way ANOVA for normalcy followed by a two tailed Student's t-test with multiple comparisons. *In vivo* animal survival data utilizes log rank statistical analyses for comparison between the survival of different treatment groups. Differences with a p-value of < 0.05 were considered statistically significant. Experiments are the means of multiple individual data points per experiment from 3 independent experiments (\pm SD).

Results

Compared to its individual component parts, as single agents or together in pairs, GZ17-6.02 was the most efficacious agent at killing prostate cancer cells (Figures 1A–C). We then performed

studies to define the biology of GZ17-6.02 and the PARP1 inhibitor olaparib alone and in combination in prostate cancer cells. GZ17-6.02 and olaparib interacted in an arithmetically greater than additive fashion with olaparib to kill prostate cancer cells (Figure 1D).

We then examined the impact of GZ17-6.02 and olaparib on cell signaling and protein expression levels in the three cell lines (Tables 2–4). Compared to prior studies in other tumor cell types such as pancreatic, liver, or colorectal, we observed significantly greater activation of ATM and the AMPK ($p < 0.05$). The phosphorylation of eIF2 α was also robustly enhanced in the prostate cancer cell lines compared to GI tumor types, yet in contrast to prior work in other tumor cell types, the phosphorylation of PKR-like endoplasmic reticulum kinase (PERK) was not significantly elevated. Other indicators of a strong ER stress response, including elevated expression of Beclin1, ATG5, and GRP78 were evident, whereas the levels of CHOP were only enhanced in PC3 cells. In all three lines, the drug combination reduced expression of HDAC2, HDAC3 and HDAC6. LNCaP and PC3 cells do not express PTEN, yet the drug combination inactivated AKT, mTOR and p70 S6K in these

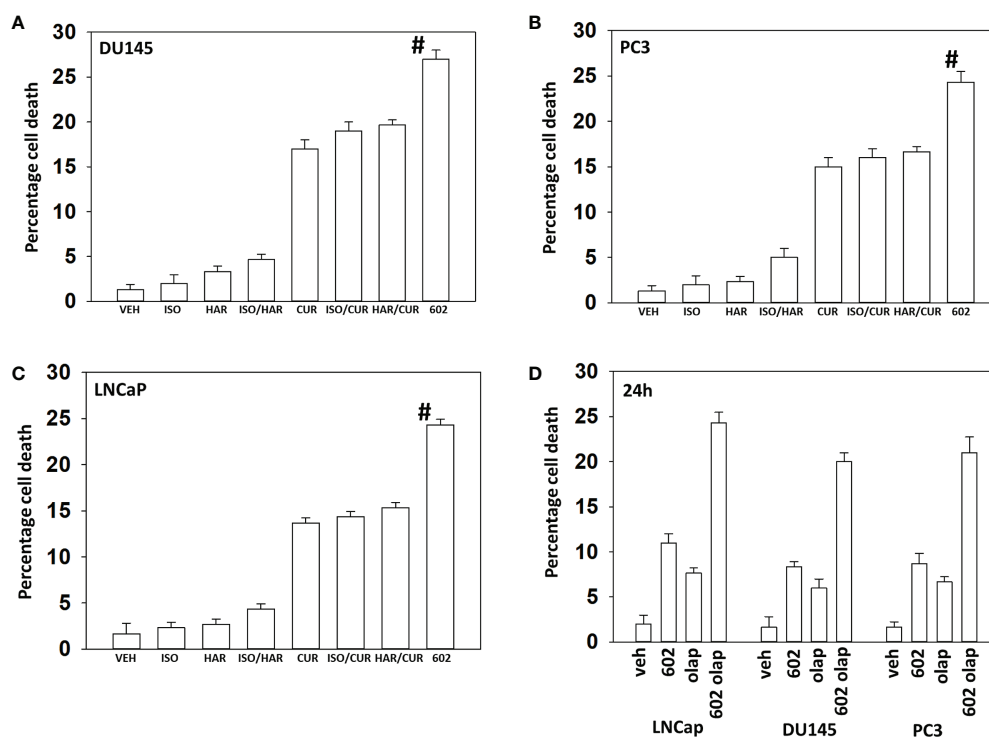


FIGURE 1

GZ17-6.02 interacts with olaparib to kill prostate cancer cells. (A–C) Prostate cancer cells were treated with vehicle control, GZ17-6.02 [curcumin (2.0 μ M) + harmine (4.5 μ M) + isovanillin (37.2 μ M)] or with component parts of GZ17-6.02 as individual agents at the indicated concentrations or in duo combinations. Cells were isolated 48h afterwards and viability determined via trypan blue exclusion assays ($n = 3 \pm$ SD). # $p < 0.05$ greater than other tested drug treatments. (D) DU145, PC3 and LNCaP prostate cancer cells were treated with vehicle control, GZ17-6.02 (2 μ M), olaparib (50 nM) or the drugs in combination for 24h. Cells were isolated, and viability determined by trypan blue exclusion. ($n = 3 \pm$ SD).

TABLE 2 Regulation of cell signaling by GZ17-6.02 and olaparib in LNCaP prostate cancer cells.

LNCaP	VEH				602				OLAPARIB				602+O						
	VEH	602	OLAPARIB	602+O	VEH	602	OLAPARIB	602+O	VEH	602	OLAPARIB	602+O	VEH	602	OLAPARIB	602+O			
6h																			
ATM	100	101	99	100	Beclin1	100	125#	112	136#	ERBB1	100	97	100	95	PD-L1	100	91	101	86*
P-ATM	100	124#	125#	142##	ATG5	100	132#	114	135#	P-ERBB1	100	96	99	97	PD-L2	100	100	101	102
AMPK	100	101	100	100	ATG13	100	100	101	102	ERBB2	100	99	99	99	MHCA	100	117#	99	120#
P-AMPK	100	121#	121#	142##	P-ATG13	100	118#	110	119#	P-ERBB2	100	90	97	86*	ODC	100	101	100	100
mTOR	100	100	99	99	GRP78	100	120#	103	131#	ERBB3	100	100	99	100	IDO1	100	103	102	104
P-mTORC1	100	88	95	83*	CHOP	100	103	94	106	P-ERBB3	100	97	103	98	p38	100	99	100	101
P-mTORC2	100	88	87*	82*	PP1	100	106	105	117#	ERBB4	100	96	98	91	P-p38	100	104	106	107
ULK1	100	100	100	98	NFkB	100	98	99	100	P-ERBB4	100	95	92	91	LATS1/2	100	99	99	100
P-ULK1 S757	100	96	99	89	P-NFkB S536	100	112	103	115#	p70 S6K	100	100	100	100	P-LATS T1097	100	109	99	123#
P-ULK1 S317	100	109	108	116#	c-SRC	100	100	100	100	P-p70 S6K T389	100	90	94	83*	P-LATS S909	100	112	101	114#
eIF2α	100	96	97	97	P-c-SRC Y416	100	85*	99	84*	PDGFRβ	100	100	100	100	YAP	100	101	101	101
P-eIF2α	100	112	108	132##	P-c-SRC Y527	100	113#	112	118#	P-PDGFRβ	100	86*	100	83*	P-YAP S127	100	111	106	122#
PERK	100	103	100	99	c-MET	100	100	100	100	ERK1/2	100	100	100	100	P-YAP S109	100	109	108	117#
P-PERK	100	105	101	111	P-c-MET	100	86*	101	84*	P-ERK1/2	100	94	99	89	P-YAP S397	100	117#	102	122#
AKT	100	100	100	99	CD95	100	101	99	100	HDAC1	100	92	99	90	TAZ	100	99	101	98
P-AKT T308	100	77*	80*	68**	FAS-L	100	105	100	109	HDAC2	100	80*	98	78*	P-TAZ S89	100	108	103	113#
STAT3	100	100	99	99	JAK2	100	99	100	100	HDAC3	100	92	95	87*	NEDD4	100	94	97	93
P-STAT3 Y705	100	87*	84*	80*	P-JAK2	100	85*	99	81*	HDAC4	100	98	99	100	PTEN	0	0	0	0
STAT5	100	100	98	99	c-KIT	100	101	101	101	HDAC5	100	102	101	101	MCL1	100	82*	97	78*
P-STAT5 Y694	100	95	98	90	P-c-KIT	100	98	98	90	HDAC6	100	86*	103	79*	BCL-XL	100	96	98	94
										HDAC7	100	96	100	95	BAX	100	99	99	99
										HDAC8	100	101	101	101	BAK	100	114#	106	117#
										HDAC9	100	100	102	101	BIM	100	113#	101	116#
										HDAC10	100	101	101	99	JNK1/2	100	101	101	110
										HDAC11	100	101	104	103	P-JNK1/2	100	115#	110	119#

LNCaP cells were treated with vehicle control, GZ17-6.02 (2 μM), olaparib (50 nM) or the drugs in combination for 6h. Cells were fixed in situ, permeabilized, stained with the indicated validated primary antibodies and imaged with secondary antibodies carrying red- and green-fluorescent tags. The staining intensity of at least 100 cells per well/condition is determined in three separate studies. The data are the normalized amount of fluorescence set at 100% comparing intensity values for vehicle control (n = 3 +/-SD). # p < 0.05 greater than vehicle control; * p < 0.05 less than vehicle; ## = greater than GZ17-6.02 as a single agent; ** = less than GZ17-6.02 as a single agent.

TABLE 3 Regulation of cell signaling by GZ17-6.02 and olaparib in PC3 prostate cancer cells.

PC3	VEH				602				OLAPARIB				602+O						
	VEH	602	OLAPARIB	602+O	VEH	602	OLAPARIB	602+O	VEH	602	OLAPARIB	602+O	VEH	602	OLAPARIB	602+O			
6h																			
ATM	100	101	101	100	Beclin1	100	12#	117#	128#	ERBB1	100	94	97	95	PD-L1	100	89	103	87*
P-ATM	100	123#	123#	140##	ATG5	100	128#	113#	134#	P-ERBB1	100	102	103	92	PD-L2	100	100	101	98
AMPK	100	98	98	97	ATG13	100	102	100	102	ERBB2	100	100	97	96	MHCA	100	121#	98	122#
P-AMPK	100	123#	122#	144##	P-ATG13	100	120#	111	126#	P-ERBB2	100	90	100	86*	ODC	100	99	101	99
mTOR	100	100	98	98	GRP78	100	113#	103	122#	ERBB3	100	99	102	94	IDO1	100	95	95	92
P-mTORC1	100	83*	96	81*	CHOP	100	116#	105	120#	P-ERBB3	100	101	107	96	p38	100	103	101	102
P-mTORC2	100	93	96	86*	PP1	100	103	101	117#	ERBB4	100	93	96	92	P-p38	100	108	110	113#
ULK1	100	101	99	102	NFkB	100	100	100	102	P-ERBB4	100	78*	96	57*	LATS1/2	100	99	97	101
P-ULK1 S757	100	90	92	86*	P-NFkB S536	100	109	101	117#	p70 S6K	100	100	101	100	P-LATS T1097	100	111	108	119#
P-ULK1 S317	100	121#	117#	129#	c-SRC	100	101	99	100	P-p70 S6K T389	100	91	99	86*	P-LATS S909	100	100	100	115#
eIF2α	100	99	100	103	P-c-SRC Y416	100	83*	95	80*	PDGFRβ	100	100	98	98	YAP	100	97	98	97
P-eIF2α	100	116#	120#	138##	P-c-SRC Y527	100	106	105	110	P-PDGFRβ	100	92	100	84*	P-YAP S127	100	107	98	109
PERK	100	97	97	97	c-MET	100	101	102	104	ERK1/2	100	100	100	100	P-YAP S109	100	103	100	106
P-PERK	100	105	102	112	P-c-MET	100	90	103	90	P-ERK1/2	100	94	97	91	P-YAP S397	100	109	97	113#
AKT	100	97	98	96	CD95	100	99	102	100	HDAC1	100	94	99	94	TAZ	100	99	102	101
P-AKT T308	100	78*	84*	74*	FAS-L	100	99	101	101	HDAC2	100	84*	96	81*	P-TAZ S89	100	110	108	119#
STAT3	100	102	103	102	JAK2	100	99	98	101	HDAC3	100	94	99	84*	NEDD4	100	91	89	84*
P-STAT3 Y705	100	86*	89	78*	P-JAK2	100	88	99	85*	HDAC4	100	99	100	99	PTEN	0	0	0	0
STAT5	100	102	101	105	c-KIT	100	98	99	101	HDAC5	100	100	103	100	MCL1	100	78*	97	76*
P-STAT5 Y694	100	95	101	93	P-c-KIT	100	96	101	94	HDAC6	100	91	101	83*	BCL-XL	100	91	100	87*
										HDAC7	100	101	101	101	BAX	100	100	96	99
										HDAC8	100	103	101	100	BAK	100	110	101	115#
										HDAC9	100	101	100	100	BIM	100	106	96	108
										HDAC10	100	99	98	100	JNK1/2	100	100	99	108
										HDAC11	100	103	100	103	P-JNK1/2	100	115#	108	119#

PC3 cells were treated with vehicle control, GZ17-6.02 (2 μM), olaparib (50 nM) or the drugs in combination for 6h. Cells were fixed in situ, permeabilized, stained with the indicated validated primary antibodies and imaged with secondary antibodies carrying red- and green-fluorescent tags. The staining intensity of at least 100 cells per well/condition is determined in three separate studies. The data are the normalized amount of fluorescence set at 100% comparing intensity values for vehicle control (n = 3 +/-SD). # p < 0.05 greater than vehicle control; * p < 0.05 less than vehicle; ## = greater than GZ17-6.02 as a single agent; ** = less than GZ17-6.02 as a single agent.

TABLE 4 Regulation of cell signaling by GZ17-6.02 and olaparib in DU145 prostate cancer cells.

DU145 6h										OLAPARIB									
	VEH	602	OLAPARIB	602+O		VEH	602	OLAPARIB	602+O		VEH	602	OLAPARIB	602+O		VEH	602	OLAPARIB	602+O
ATM	100	100	100	100	Beclin1	100	128#	115#	132#	ERBB1	100	94	95	99	PD-L1	100	88	93	86*
P-ATM	100	121#	124#	140##	ATG5	100	134#	112#	137#	P-ERBB1	100	87*	91	86*	PD-L2	100	84	89	85*
AMPK	100	100	100	100	ATG13	100	100	101	98	ERBB2	100	100	100	100	MHCA	100	111	109	114#
P-AMPK	100	117#	120#	138##	P-ATG13	100	116#	107	118#	P-ERBB2	100	95	98	95	ODC	100	100	100	100
mTOR	100	100	100	100	GRP78	100	118#	102	127#	ERBB3	100	104	103	105	IDO1	100	102	101	99
P-mTORC1	100	90	97	86*	CHOP	100	104	90	105	P-ERBB3	100	104	101	107	p38	100	102	101	101
P-mTORC2	100	88	97	80*	PP1	100	114#	107	117#	ERBB4	100	98	110	104	P-p38	100	99	100	101
ULK1	100	100	100	100	NFkB	100	99	101	98	P-ERBB4	100	90	94	86*	LATS1/2	100	99	99	100
P-ULK1 S757	100	92	95	86*	P-NFkB S536	100	112	99	116#	p70 S6K	100	99	102	99	P-LATS T1097	100	99	101	114#
P-ULK1 S317	100	116#	117#	119#	c-SRC	100	101	97	102	PDGFRβ	100	98	97	96	P-LATS S909	100	99	98	109
eIF2α	100	97	98	98	P-c-SRC Y416	100	85*	98	82*	P-PDGFRβ	100	95	97	84*	YAP	100	99	100	98
P-eIF2α	100	113#	110	131##	P-c-SRC Y527	100	103	104	110	ERK1/2	100	100	100	100	P-YAP S127	100	109	102	112
PERK	100	103	99	100	c-MET	100	99	99	102	P-ERK1/2	100	91	97	84*	P-YAP S109	100	102	101	111
P-PERK	100	103	100	110	P-c-MET	100	85*	101	85*	HDAC1	100	86*	96	86*	P-YAP S397	100	99	100	107
AKT	100	99	100	100	CD95	100	98	100	100	HDAC2	100	86	102	86*	TAZ	100	99	99	100
P-AKT T308	100	77*	88	73*	FAS-L	100	102	99	100	HDAC3	100	94	95	85*	P-TAZ S589	100	110	107	113#
STAT3	100	99	100	100	JAK2	100	102	102	101	HDAC4	100	98	99	97	NEDD4	100	94	96	85*
P-STAT3 Y705	100	85*	96	76*	P-JAK2	100	98	97	84*	HDAC5	100	97	100	98	PTEN	100	99	99	99
STAT5	100	101	100	99	c-KIT	100	100	101	100	HDAC6	100	90	97	78*	MCL1	100	84*	98	80*
P-STAT5 Y694	100	97	99	97	P-c-KIT	100	101	99	96	HDAC7	100	100	101	97	BCL-XL	100	93	98	83*
										HDAC8	100	102	102	101	BAK	0	0	0	0
										HDAC9	100	99	99	98	BAK	100	111	99	116#
										HDAC10	100	101	100	99	BIM	100	111	103	114#
										HDAC11	100	99	102	100	JNK1/2	100	102	100	102
															P-JNK1/2	100	111	106	113#

DU145 cells were treated with vehicle control, GZ17-6.02 (2 μM), olaparib (50 nM) or the drugs in combination for 6h. Cells were fixed in situ, permeabilized, stained with the indicated validated primary antibodies and imaged with secondary antibodies carrying red- and green-fluorescent tags. The staining intensity of at least 100 cells per well/condition is determined in three separate studies. The data are the normalized amount of fluorescence set at 100% comparing intensity values for vehicle control (n = 3 +/-SD). # p < 0.05 greater than vehicle control; * p < 0.05 less than vehicle. ## = greater than GZ17-6.02 as a single agent; ** = less than GZ17-6.02 as a single agent.

lines as well as in DU145 cells. Unlike other tumor cell types previously tested, in all three prostate lines, the drug combination significantly enhanced activity in the c-Jun NH2-terminal kinase (JNK) pathway.

We next performed molecular studies to link the cause-and-effect of cell signaling processes outlined in Figures 2–4. Knock down of ATM significantly reduced the ability of the drug combination to increase phosphorylation of AMPKα T172 and ULK1 S317, and to decrease the phosphorylation of ULK1 S757, mTOR S2448 and mTOR S2481 (Figure 2). In agreement with these changes in protein phosphorylation, knock down of ATM or of the AMPKα significantly reduced autophagosome formation and reduced levels of autophagic flux (Figure 3). Knock down of AMPKα prevented the drug combination from altering the phosphorylation of ULK1 or mTOR (Figure 4). Thus, GZ17-6.02-induced ATM-AMPK signaling regulates the activities of ULK1 and mTOR.

Knock down of eIF2α reduced the abilities of GZ17-6.02 and olaparib to increase autophagosome formation and to flux into autolysosomes and knock down of eIF2α significantly reduced the ability of GZ17-6.02 alone or in combination with olaparib to increase Beclin1 and ATG5 expression, proteins that are essential for autophagosome formation (Figures 5A, B). In Table 2, although drug exposure significantly increased eIF2α S51 phosphorylation, PERK was not significantly activated and hence we determined the most likely kinase(s) regulating eIF2α S51 phosphorylation in prostate cancer cells. There are several

other well-described kinases that catalyze the phosphorylation of eIF2α S51, including the interferon-induced, double-stranded RNA-activated protein kinase, known as protein kinase R (PKR); general control non-derepressible 2 (GCN2); and heme-regulated eIF2α kinase (HRI) (14, 15). Across all three cell lines tested, only knock down of PKR significantly reduced the drug-induced enhancement of eIF2α S51 phosphorylation (Figure 5C).

Signaling by PKR can activate the JNK1/2 MAPK pathway. As eIF2α S51 phosphorylation was predominantly mediated by PKR in prostate cancer cells, and that we had unexpectedly observed activation of the JNK1/2 pathway in prostate cancer cells, we determined whether the JNK1/2 pathway was being regulated by GZ17-6.02 via a PKR-dependent mechanism. Knock down of PKR reduced the basal activity of the JNK1/2 pathway by ~20% and knock down of PKR largely prevented the drug combination from activating JNK1/2 (Figure 6A). Treatment of cells with the cell-permeable JNK-inhibitory peptide significantly reduced the lethality of the drug combination (Figure 6B). Knock down of PKR significantly reduced the lethality of the drug combination (Figure 7A). Knock down of PKR also reduced the amount of drug-induced autophagosome formation but did not block autophagic flux (Figure 7B).

We then defined the impact of knocking down eIF2α expression on the abilities of GZ17-6.02 and olaparib to activate ATM and the AMPK. Knock down of eIF2α unexpectedly reduced the basal protein expression levels of

6h	VEH	6+O	VEH	6+O	VEH	6+O	VEH	6+O	VEH	6+O	VEH	6+O	VEH	6+O
DU145	100	98	100	139#	99	102	97	107	100	100	100	100	100	100
PC3	100	99	100	145#	98	101	102	110	100	100	100	100	100	100
LNCaP	100	99	100	134#	101	100	99	104	100	99	100	100	100	100
	AMPK α		P-AMPK α		AMPK α		P-AMPK α		siSCR		siATM		ERK2	
	siSCR				siATM									
	VEH	6+O	VEH	6+O	VEH	6+O	VEH	6+O	VEH	6+O	VEH	6+O	VEH	6+O
DU145	100	99	100	83*	100	119#	99	99	100	95	100	106	100	106
PC3	100	100	100	87*	100	116#	100	101	99	92	99	102	99	102
LNCaP	100	101	100	85*	100	114#	101	101	97	92	100	105	100	105
	ULK1		P-S757		P-317		ULK1		P-S757		P-317			
	siSCR				siATM									
	VEH	6+O	VEH	6+O	VEH	6+O	VEH	6+O	VEH	6+O	VEH	6+O	VEH	6+O
DU145	100	101	100	82*	100	81*	100	100	103	98	99	98	99	98
PC3	100	99	100	86*	100	84*	99	99	99	93	99	92	99	92
LNCaP	100	101	100	84*	100	86*	101	101	99	95	99	95	99	95
	mTOR		P-S2448		P-2481		mTOR		P-S2448		P-2481			
	siSCR				siATM									

FIGURE 2

Regulation of AMPK, ULK1 and mTOR by [GZ17-6.02 + olaparib] requires ATM. Cells were transfected with a scrambled siRNA or with an siRNA to knock down expression of ATM. After 24h, cells were treated with vehicle control or [GZ17-6.02 (2 μ M) and olaparib (50 nM)] in combination for 6h. Cells were fixed in situ, permeabilized, stained with the indicated validated primary antibodies and imaged with secondary antibodies carrying red- and green-fluorescent tags. The staining intensity of at least 100 cells per well/condition is determined in three separate studies. The graphical data presented are the normalized amount of fluorescence set at 100% comparing intensity values for vehicle control (n = 3 +/-SD). # p < 0.05 greater than vehicle control; * p < 0.05 less than vehicle control.

both ATM and AMPK α (Figure 8). However, knock down of eIF2 α did not alter the *relative ability* of the drugs to cause ATM and AMPK activation or inactivation of residual eIF2 α itself. Knock down of eIF2 α reduced the ability of GZ17-6.02 as a single agent and when combined with olaparib to significantly increase GRP78 levels, although a trend was evident arguing loss of eIF2 α did not fully block the induction of GRP78 (Figure 9). The enhanced GRP78 expression was localized in punctate bodies in the cytoplasm of the tumor cells (not shown).

We then determined whether knock down of ATM or AMPK α altered the drug-induced increase in eIF2 α S51 phosphorylation. Knock down of either ATM or AMPK α significantly reduced the ability of the drug combination to enhance phosphorylation of eIF2 α S51 (Figure 10A). Based on our findings in Figures 4-6A, we determined whether knock down of ATM altered the basal expression of PKR. Knock down of ATM neither altered PKR expression nor its phosphorylation (Figure 10B). Thus, in prostate cancer cells eIF2 α controls basal ATM and AMPK α protein levels and that in the absence of ATM or AMPK, the ability of the cell to cause eIF2 α S51 phosphorylation is also diminished.

Additional studies then determined the relative importance of signaling proteins in tumor cell killing caused by the drug combination. Over-expression of BCL-XL or knock down of toxic BH3 domain proteins reduced killing, as did to a lesser extent knock down of CD95 or FADD (Figure 11). Over-

expression of the caspase 8/10 inhibitor FLIP-s was significantly more protective than knock down of CD95 or FADD implying in our system caspase 8/10 was a component of an amplification loop in the cell killing process. Knock down of eIF2 α , Beclin1 or ATG5 also reduced tumor cell death to a similar extent as did over-expression of FLIP-s whereas knock down of ATM less effective. Knock down of eIF2 α was more cytoprotective than knock down of PKR (Figures 6A, 11). Compiling data for the three lines, we observed in Figure 5 that knock down of eIF2 α reduced autophagosome formation by ~25% whereas in Figure 11, knock down of eIF2 α reduced tumor cell killing by ~70%, as did knock down of Beclin1 or ATG5 (\ddagger p < 0.05).

Based on the key role ATM signaling was playing in the regulation of ER stress signaling and tumor cell viability, we defined the localization of activated ATM, caused by exposure to GZ17-6.02. Within 30 min of exposure, the phosphorylation of ATM S1981 was increased (Figure 12). Increased staining was peri-nuclear. The total expression of ATM data did not change (not shown). We then examined the localization of phosphorylated ATM S1981 6h after treatment with GZ17-6.02. Although the majority of ATM protein was localized in the peri-nuclear region, phosphorylated ATM S1981 was localized in the nucleus (Figure 13). Within 6h of exposure, GZ17-6.02 had reduced the expression of RAD51 (Figure 14A). This data argues that the initial activation of ATM outside the

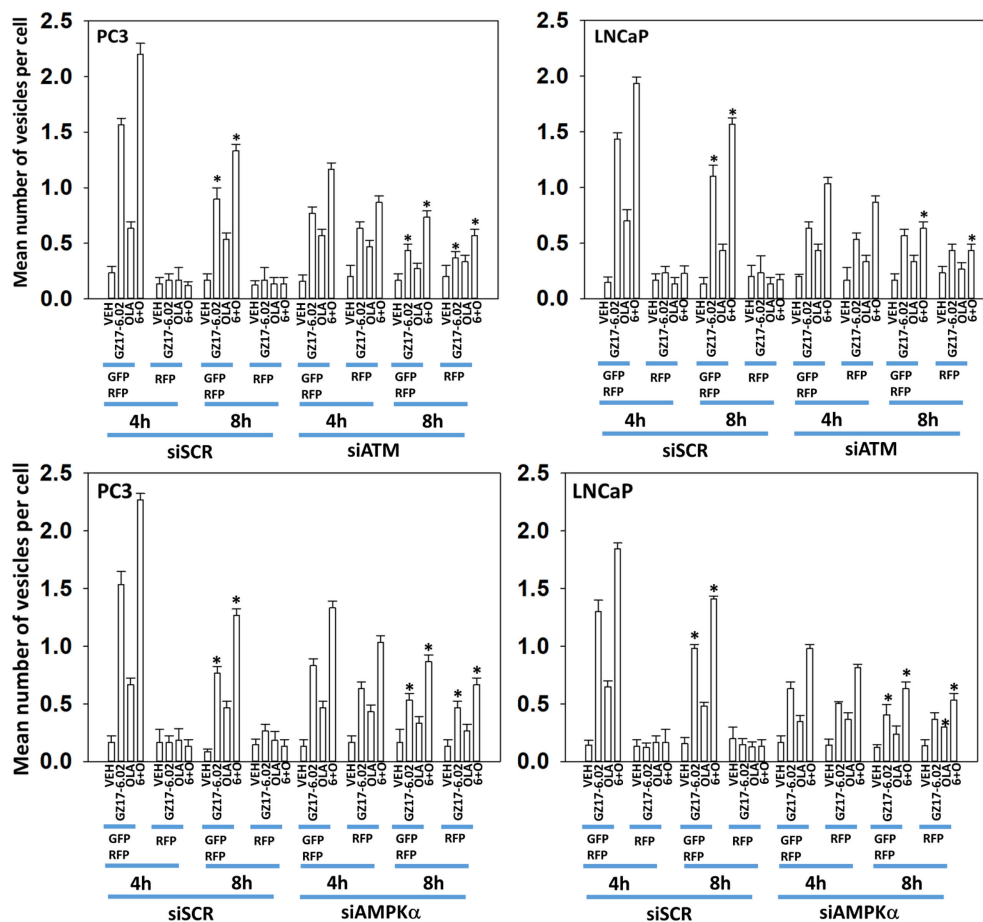


FIGURE 3

Knock down of ATM reduces autophagosome formation and autophagic flux. PC3 and LNCaP cells were transfected with a plasmid to express LC3-GFP-RFP and in parallel transfected with a scrambled siRNA or with siRNA molecules to knock down the expression of ATM or of AMPK α . Twenty-four h later, cells were treated with vehicle control, GZ17-6.02 (2 μ M), olaparib (50 nM) or the drugs in combination for 4h and 8h. At each time point, the mean number of GFP+RFP+ and only RFP+ vesicles per cell were determined (n = 3 +/-SD). * p < 0.05 less than corresponding value in siSCR transfected cells.

nucleus reduces the expression of RAD51 which results in enhanced DNA damage in the nucleus and with activation of nuclear ATM. We then performed Comet assays to assess the amount of DNA damage being caused by the drugs alone or in combination. In comparison to GZ17-6.02, olaparib caused only modest levels of DNA damage (Figure 14B). The combination of GZ17-6.02 and olaparib caused greater amounts of DNA damage than treatment with GZ17-6.02 as a single agent.

Finally, we determined whether GZ17-6.02 and olaparib interacted *in vivo* to suppress the growth of LNCaP tumors. As a single agent, GZ17-6.02 profoundly suppressed LNCaP tumor growth and prolonged animal survival (Figures 15A, B). As a single agent, olaparib more modestly reduced tumor growth, and also prolonged survival. The drugs in combination caused an additional smaller significant reduction in tumor growth that became particularly evident at ~days 35-40

and became even more obvious following discontinuation of drug treatment at day 45. However, there was no significant enhancement in survival comparing mice treated with GZ17-6.02 or with GZ17-6.02 and olaparib. Animal body mass under all treatment conditions did not significantly change over the 45-day time course (Figure 15C). Our data support the use of GZ17-6.02 as a therapeutic agent in patients with AR+ prostate cancer.

Discussion

The present studies demonstrated that GZ17-6.02 interacted with the PARP1 inhibitor olaparib to kill prostate cancer cells. The lethal interaction between the drugs occurred regardless of whether the cells lacked expression of PTEN or had inactivating mutations in BRCA1/2. Multiple cell death effector pathways

		6h						6h					
		VEH	6+O	VEH	6+O	VEH	6+O	VEH	6+O	VEH	6+O	VEH	6+O
DU145		100	99	100	83*	100	118#	99	98	105	100	100	107
PC3		100	103	100	86*	100	118#	99	99	100	96	100	103
LNCaP		100	101	100	85*	100	117#	101	100	101	96	104	101
		ULK1		P-S757		P-317		ULK1		P-S757		P-317	
		siSCR						siAMPK α					

		6h						6h						6h					
		VEH	6+O	VEH	6+O	VEH	6+O	VEH	6+O	VEH	6+O	VEH	6+O	VEH	6+O	VEH	6+O		
DU145		100	101	100	83*	100	78*	100	99	95	93	105	106	100	101	101	100		
PC3		100	100	100	87*	100	82*	98	98	99	94	98	90	100	100	100	100		
LNCaP		100	100	100	84*	100	83*	100	100	98	94	95	91	100	100	100	100		
		mTOR		P-S2448		P-2481		mTOR		P-S2448		P-2481		siSCR		siAMPK α			
		siSCR						siAMPK α						ERK2					

FIGURE 4

Regulation of ULK1 and mTOR by [GZ17-6.02 + olaparib] requires the AMPK. Cells were transfected with a scrambled siRNA or with an siRNA to knock down expression of AMPK α . After 24h, cells were treated with vehicle control or [GZ17-6.02 (2 μ M) and olaparib (50 nM)] in combination for 6h. Cells were fixed in situ, permeabilized, stained with the indicated validated primary antibodies and imaged with secondary antibodies carrying red- and green-fluorescent tags. The staining intensity of at least 100 cells per well/condition is determined in three separate studies. The data are the normalized amount of fluorescence set at 100% comparing intensity values for vehicle control (n = 3 +/-SD). # p < 0.05 greater than vehicle control; *p < 0.05 less than vehicle control.

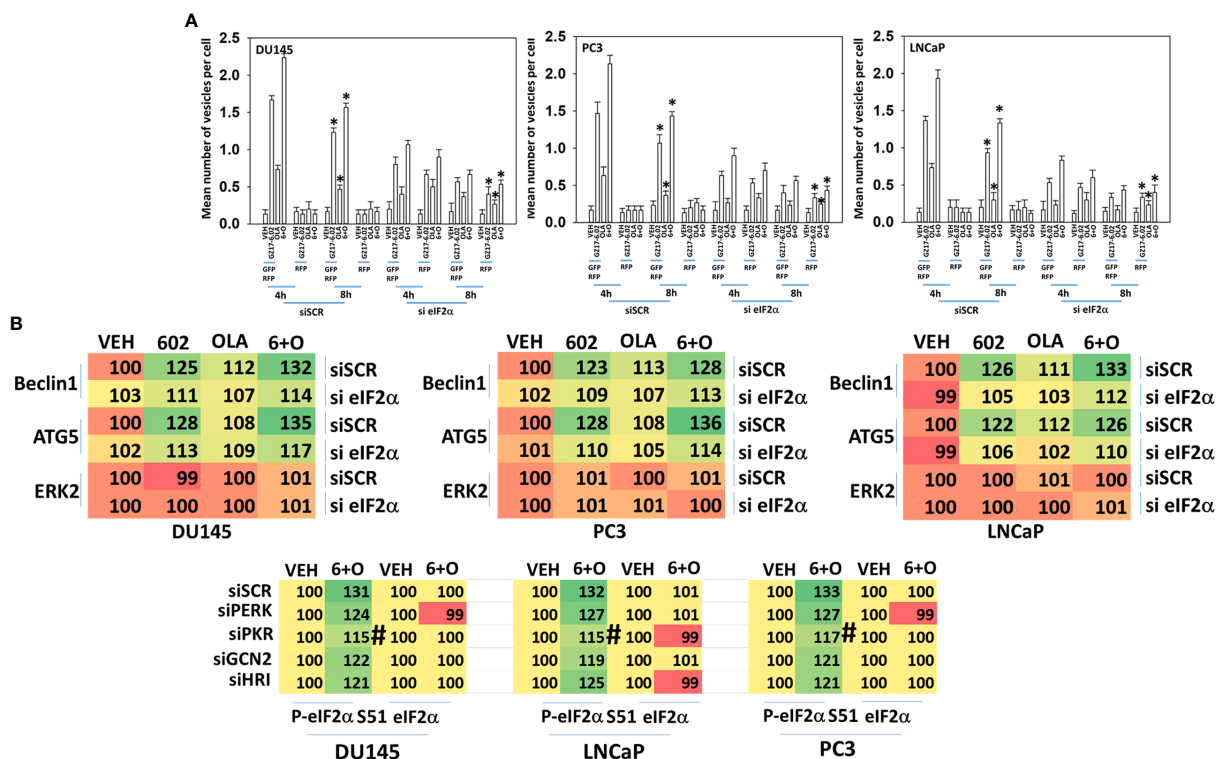
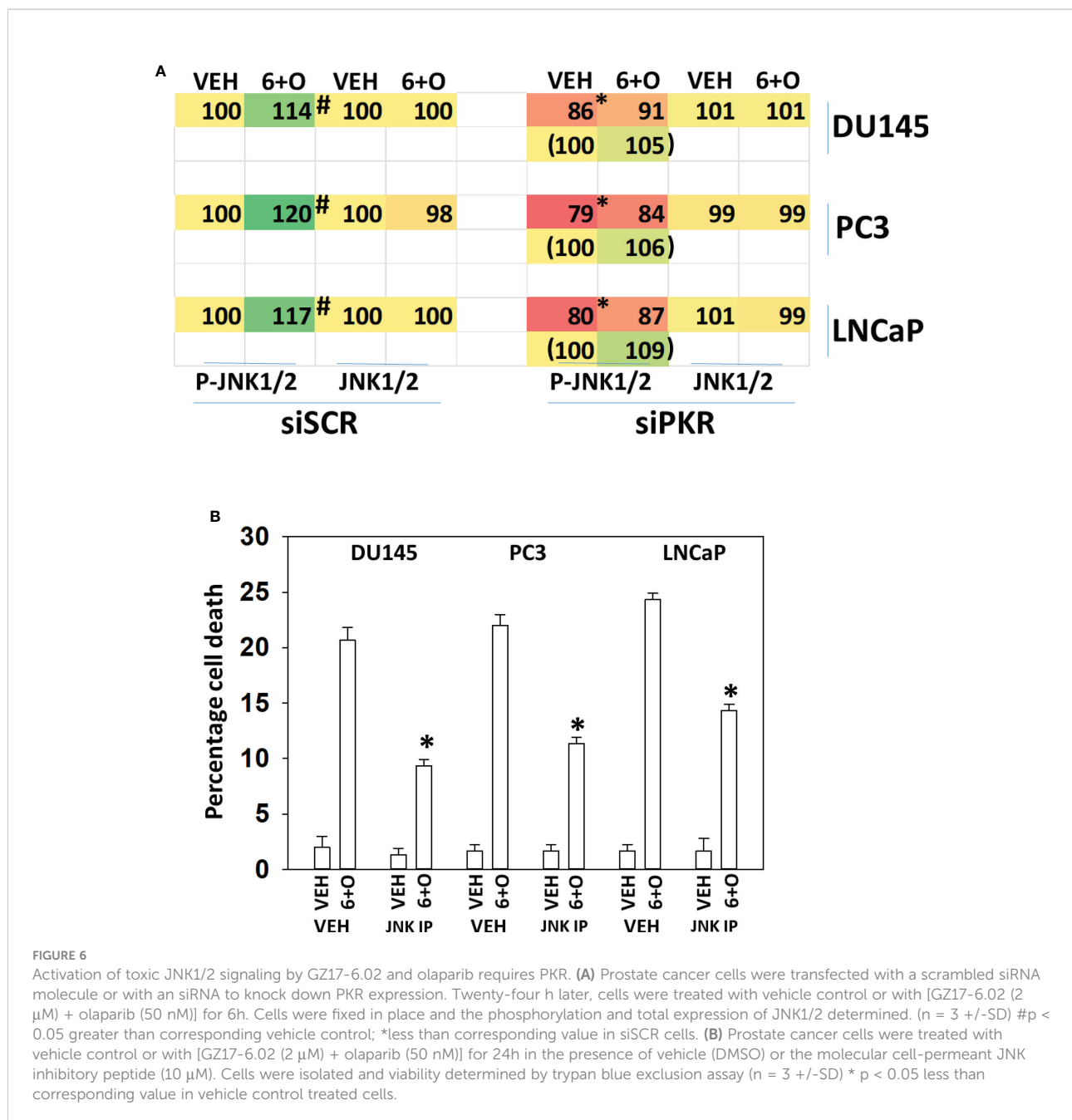


FIGURE 5

ER stress signaling is required for autophagosome formation and the increased expression of Beclin1 and ATG5. (A) Cells were transfected with a plasmid to express LC3-GFP-RFP and in parallel transfected with a scrambled siRNA or with an siRNA to knock down the expression of eIF2 α . Twenty-four h later, cells were treated with vehicle control, GZ17-6.02 (2 μ M), olaparib (50 nM) or the drugs in combination for 4h and 8h. At each time point, the mean number of GFP+RFP+ and only RFP+ vesicles per cell were determined (n = 3 +/-SD). *p < 0.05 less than corresponding value in siSCR transfected cells. (B) Cells were transfected with a scrambled siRNA or with an siRNA to knock down the expression of eIF2 α . Twenty-four h later, cells were treated with vehicle control, GZ17-6.02 (2 μ M), olaparib (50 nM) or the drugs in combination for 6h. Cells were fixed in situ, permeabilized, stained with the indicated validated primary antibodies and imaged with secondary antibodies carrying red- and green-fluorescent tags. The staining intensity of at least 100 cells per well/condition is determined in three separate studies. The data presented the normalized amount of fluorescence set at 100% comparing intensity values for vehicle control (n = 3 +/-SD). # p < 0.05 greater than vehicle control; *p < 0.05 less than vehicle control; † p < 0.05 less than corresponding value in siSCR cells.



were engaged by the drug combination, in particular toxic autophagosome formation and death receptor signaling, both leading to mitochondrial dysfunction with mixed apoptotic and non-apoptotic killing. Upstream initiators of drug action were activation of ATM-AMPK signaling and increased endoplasmic reticulum stress signaling *via* PKR and eIF2 α .

Compared to other solid tumor cell types we have previously tested, the activation of ATM caused by GZ17-6.02 was significantly greater in prostate cancer cells. And, furthermore, the activation of ATM was prolonged when compared to other

tumor types. In HCT116 colon cancer cells we had previously found within 1h of GZ17-6.02 exposure that the expression of XPA and XPD had declined and the levels of RAD51 and RAD52 were enhanced (1). At this early timepoint, neither RAD51 nor RAD52 colocalized with nuclear P- γ H2AX staining, and instead, RAD51 and RAD52 were predominantly found in the perinuclear space. In support of those earlier observations, we discovered in prostate cancer cells that different pools of ATM protein were being activated at different time points. One hour following GZ17-6.02

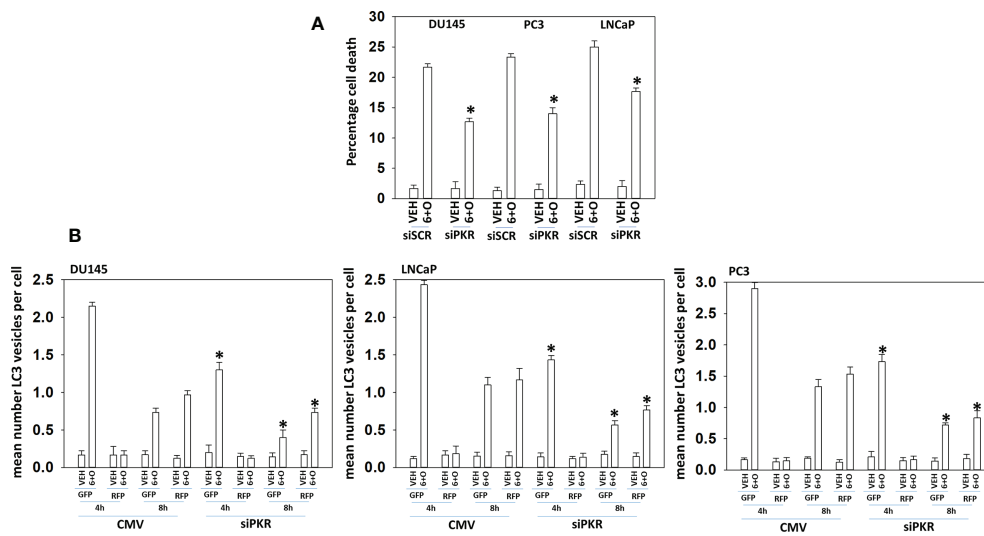


FIGURE 7 Signaling by PKR is required for tumor cell killing and autophagosome formation. **(A)** Prostate cancer cells were transfected with a scrambled siRNA or with an siRNA to knock down the expression of PKR. Twenty-four h later, cells were treated with vehicle control or with [GZ17-6.02 (2 μM) + olaparib (50 nM)] for 24h. Cells were isolated, and viability determined by trypan blue exclusion assay (n = 3 +/-SD). *p < 0.05 less than corresponding value in vehicle control treated cells. **(B)** Prostate cancer cells were transfected with a scrambled siRNA or with an siRNA to knock down the expression of PKR and in parallel transfected with a plasmid to express LC3-GFP-RFP. Twenty-four h later, cells were treated with vehicle control, GZ17-6.02 (2 μM), olaparib (50 nM) or the drugs in combination for 4h and 8h. At each time point, the mean number of GFP+RFP+ and only RFP+ vesicles per cell were determined (n = 3 +/-SD). *p < 0.05 less than corresponding value in siSCR transfected cells.

treatment, ATM in the perinuclear space was activated whereas after 6h of exposure, ATM within the nucleus itself was phosphorylated. ATM outside of the nucleus has been argued to be regulated by reactive oxygen species however, our data in HCT116 cells demonstrated that ROS was not a component of GZ17-6.02 biology (6). In prostate cancer cells the expression of

the DNA repair protein RAD51 was reduced by GZ17-6.02 after 6h of exposure and that DNA damage measured *via* comet assays persisted for up to at least 6h. The complicated molecular mechanisms by which GZ17-6.02 regulates ATM function outside and inside the nucleus, and DNA damage signaling, and repair will require studies beyond the present manuscript.

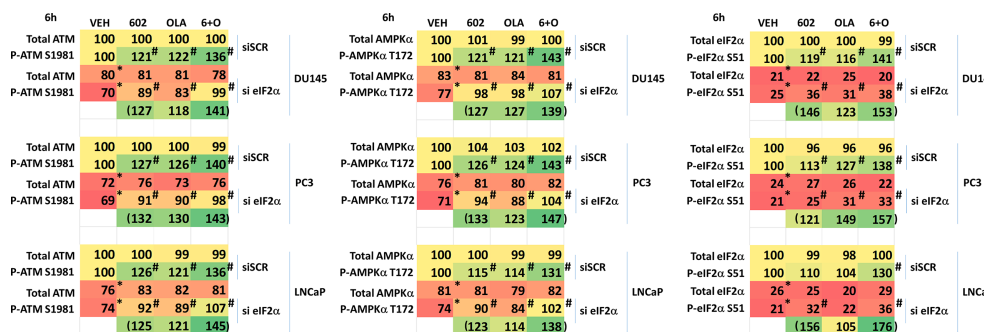


FIGURE 8 Activation of ATM and the AMPK by GZ17-6.02 alone or in combination with olaparib requires ER stress signaling. Cells were transfected with a scrambled siRNA or with an siRNA to knock down the expression of eIF2α. After 24h, cells were treated with vehicle control, GZ17-6.02 (2 μM), olaparib (50 nM) or the drugs in combination for 6h. Cells were fixed in situ, permeabilized, stained with the indicated validated primary antibodies and imaged with secondary antibodies carrying red- and green-fluorescent tags. The staining intensity of at least 100 cells per well/condition is determined in three separate studies. The data are the normalized amount of fluorescence set at 100% comparing intensity values for vehicle control (n = 3 +/-SD). #p < 0.05 greater than vehicle control, *p < 0.05 less than vehicle control.

	siSCR				si eIF2 α				
	VEH	602	OLA	6+O	VEH	602	OLA	6+O	
GRP78	100	113 [#]	101	118 [#]	92	103	94	102	DU145
					(112	102	111)		
GRP78	100	114 [#]	100	118 [#]	95	103	96	106	PC3
					(109	101	111)		
GRP78	100	118 [#]	105	124 [#]	99	111	100	114	LNCaP
					(112	101	115)		

FIGURE 9

Increased expression of GRP78 caused by GZ17-6.02 alone or in combination with olaparib requires ER stress signaling. Cells were transfected with a scrambled siRNA or with an siRNA to knock down the expression of eIF2 α . After 24h, cells were treated with vehicle control, GZ17-6.02 (2 μ M), olaparib (50 nM) or the drugs in combination for 6h. Cells were fixed in situ, permeabilized, stained with the indicated validated primary antibodies and imaged with secondary antibodies carrying red- and green-fluorescent tags. The staining intensity of at least 100 cells per well/condition is determined in three separate studies. The data are the normalized amount of fluorescence set at 100% comparing intensity values for vehicle control (n = 3 +/-SD). #p < 0.05 greater than vehicle control; *p < 0.05 less than vehicle control.

In other tumor cell types, GZ17-6.02 was shown to significantly activate PERK, which was responsible for drug-induced phosphorylation of serine 51 and inactivation of eIF2 α . It was therefore unexpected when we discovered that in prostate cancer cells GZ17-6.02 did not significantly activate PERK, although the drug was still competent to significantly enhance eIF2 α S51 phosphorylation. There are multiple kinases recognized to catalyze the phosphorylation of eIF2 α S51 including PKR, GCN2 and HRI. Knock down of PKR, but not of PERK, GCN2 or HRI significantly reduced the ability of the drug combination to enhance S51 phosphorylation (14, 15).

Interferon-induced, double-stranded RNA-activated protein kinase (PKR), is a universally and constitutively expressed serine-threonine kinase with well-described roles in the regulation of immunity, metabolism, and neurological diseases (16–19). PKR signaling, *via* activation of the JNK MAPK pathway, has been linked to increased expression of inflammatory cytokines such as IL-1 β and TNF α . Twenty years ago, we explored the Janus-faced nature of JNK signaling (20). In primary hepatocytes treated with a bile acid JNK signaling had the potential to both promote G1 progression and under different signaling circumstances, hepatocyte cell death. In prostate cancer cells, a similar situation has been reported. For example, inhibition of MEK4/7 and/or JNK1/2 reduced proliferation and invasion, presumably due to dephosphorylation of c-Jun and inactivation of AP-1 signaling complexes (21, 22). However, paclitaxel toxicity in prostate cancer cells requires activation of JNK (23). Unlike in other types of tumor cell, GZ17-6.02 and olaparib caused a robust activation of JNK1/2 and knock down of PKR prevented this response (1). PKR can activate the transcription factor NF κ B (18). In other tumor types, we observed either no effect or inactivation of NF κ B signaling caused by GZ17-6.02 whereas in prostate cancer cells,

the drugs in combination activated NF κ B. Activation of NF κ B signaling in prostate cancer is most often linked to increased proliferation and tumor development (24, 25). However, expression of a constitutively active form of p65 NF κ B causes apoptosis in prostate cancer cells, in part due to increased expression of the death receptor CD95 (FAS) and enhanced levels of toxic BH3 domain proteins (26). Future studies will be required to link signaling by PKR, through to JNK and NF κ B signaling, and to the inflammatory microenvironment in prostate cancer tumors treated with GZ17-6.02 and olaparib.

One of the first manuscripts published examining the biology of GZ17-6.02 linked its effects on pancreatic cancer cells to the regulation of super-enhancers (SEs) (27). SEs are specialized areas of the genome which drive high rates of transcription and play a key role in cell biology. Using CHIP-Seq, it was discovered that GZ17-6.02 altered the acetylation of the genes, lowered the activities of major transcription factors and stem cell markers. GZ17-6.02 reduced both Oct-4 expression and decreased in the occupancy of OCT-4 in the entire genome. In prostate cancer, SEs force the tumor cells to become addicted to dysregulated transcription programs mediated by proteins such as BRD4, CDK7, and ERG (28–30). Whether GZ17-6.02 can regulate SEs in prostate cancer, and link altered transcription to the biology described herein will require studies beyond the scope of this paper.

There remains in the cancer therapeutics field a controversy as to the relevance of autophagy either in reducing the efficacy of therapeutic regimens or playing an active role in the tumor cell killing process. We discovered that knock down of eIF2 α was more cytoprotective than knock down of PKR, suggesting that PKR is not the only eIF2 α kinase playing a regulatory role in our system. Compiling and comparing the data from the three lines we examined, we determined that knock down of eIF2 α reduced

A

6h	VEH	6+O	VEH	6+O	VEH	6+O	VEH	6+O
DU145	100	100	100	128#	100	100	98	109
PC3	100	100	100	123#	99	100	101	108
LNCaP	100	102	100	126#	101	101	102	108
	siSCR				siATM			
P-eIF2 α S51								

	VEH	6+O	VEH	6+O	VEH	6+O	VEH	6+O
DU145	100	99	100	128#	95	94	100	110
PC3	100	100	100	124#	99	99	100	107
LNCaP	100	101	100	126#	100	101	102	110
	siSCR				siAMPK α			
P-eIF2 α S51								

B

	PKR		P-PKR	
DU145	100	100	100	95
PC3	100	100	100	96
LNCaP	100	100	100	94
	siSCR		siATM	

FIGURE 10

Knock down of ATM or AMPK α reduces the ability of [GZ17-6.02 + olaparib] to increase eIF2 α S51 phosphorylation. (A) Cells were transfected with a scrambled siRNA control or with siRNA molecules to knock down the expression of either ATM or AMPK α . After 24h, cells were treated with vehicle control or with [GZ17-6.02 (2 μ M) and olaparib (50 nM)] in combination for 6h. Cells were fixed in situ, permeabilized, stained with the indicated validated primary antibodies and imaged with secondary antibodies carrying red- and green-fluorescent tags. The staining intensity of at least 100 cells per well/condition is determined in three separate studies. The data are the normalized amount of fluorescence set at 100% comparing intensity values for vehicle control (n = 3 +/-SD). #p < 0.05 greater than vehicle control; *p < 0.05 less than vehicle control. (B) Cells were transfected with a scrambled siRNA control or with siRNA molecules to knock down the expression of ATM or AMPK α . After 24h, cells were fixed in place and staining for PKR and ERK2 as a loading control performed (n = 3 +/-SD) * p < 0.05 less than siSCR control.

autophagosome formation by only ~25% whereas knock down of eIF2 α reduced tumor cell killing to a significantly greater extent, ~70%. In comparison, knock down of either Beclin1 or ATG5 reduced both autophagy and cell killing by ~70%. Thus, inhibition of autophagy by only ~25% is sufficient to reduce killing by ~70%. This suggests that above a certain threshold, estimated to be ~75% of the total expected autophagosome formation, the GZ17.602 olaparib drug combination causes autophagy to become toxic. And, to achieve the higher toxic level of autophagosome formation and autophagic flux, ER stress signaling, i.e., eIF2 α inactivation, must be intact.

Although we do not know how much inhibition of PARP is caused by 10 mg/kg in a mouse tumor, prior studies in patients have been performed. With a 400 mg BID olaparib dosing schedule, pharmacokinetic (PK) investigations demonstrated a rapid

absorption of olaparib (peak plasma concentration was between 1 and 3 h after dosing) and elimination (terminal-elimination with a half-life of ~5 to ~7 h) of olaparib (31, 32). Pharmacodynamic (PD) assessments demonstrated PARP inhibition in surrogate samples; peripheral blood mononuclear cells (PBMCs), and tumor tissue. These studies revealed that PARP inhibition in PBMCs rapidly reached a plateau of approximately sixty percent.

GZ17-6.02 is undergoing phase I evaluation in cancer patients. Hence, in addition to our *in vitro* mechanistic analyses, we performed *in vivo* studies to define the *in vivo* interaction between GZ17-6.02 and olaparib. Our *in vivo* data argue that GZ17-6.02 may have single agent potential to suppress the growth of AR+ prostate cancer tumors and prolong survival. Although GZ17-6.02 and olaparib interacted to suppress growth below that of GZ17-6.02 as a single agent, in the absence of drugs, the tumors

24h

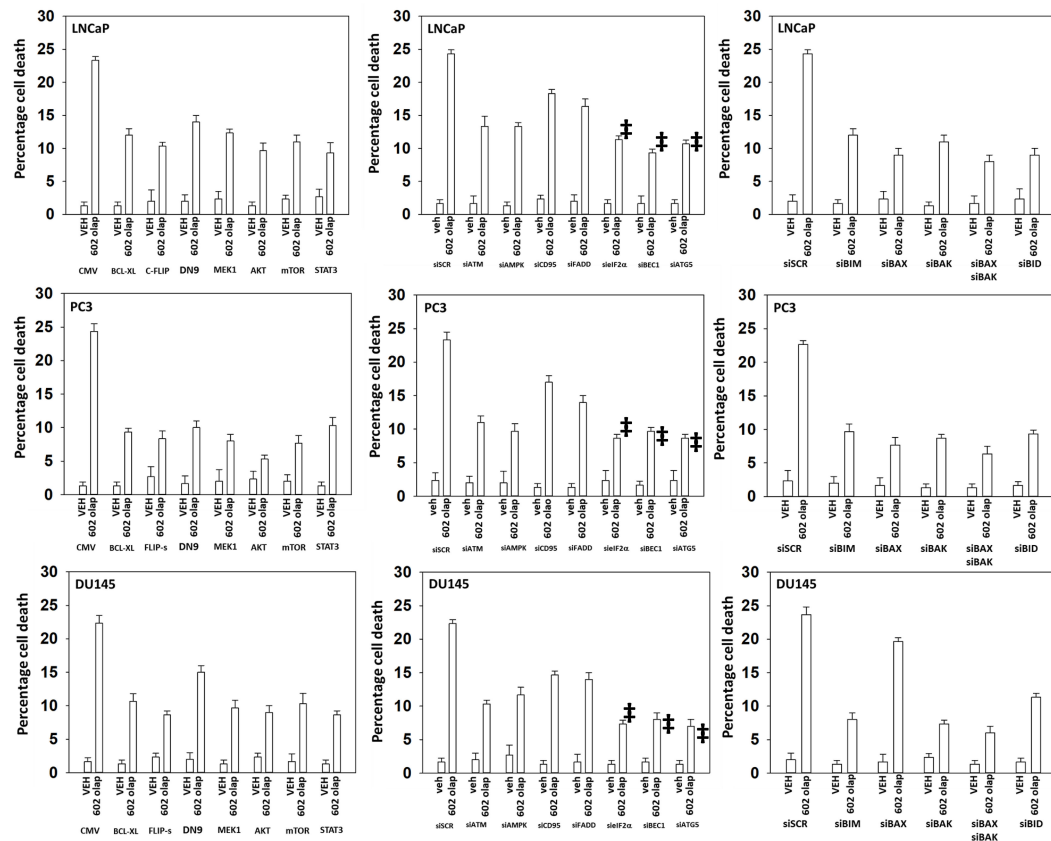


FIGURE 11

Knock down of Beclin1, ATG5 or eIF2 α , or over-expression of FLIP-s significantly reduces the lethality of [GZ17-6.02 + olaparib]. Prostate cancer cells were transfected with an empty vector plasmid or with plasmids to express BCL-XL, FLIP-s, dominant negative caspase 9, activated MEK1, activated AKT, activated mTOR or activated STAT3. Cells were transfected with a scrambled siRNA or with siRNA molecules to knock down the expression of ATM, AMPK α , CD95, FADD, eIF2 α , Beclin1, ATG5, BIM, BAX, BAK and BID. After 24h, cells were treated with vehicle control or with [GZ17-6.02 (2 μ M) and olaparib (50 nM)] in combination for 24h. Cells were isolated, and viability determined by trypan blue exclusion. (n = 3 +/- SD). #p < 0.05 less than corresponding value in siATM or siAMPK α cells.

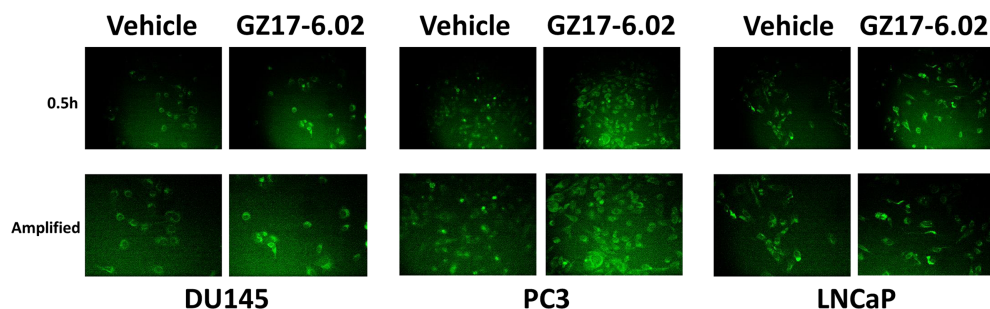


FIGURE 12

GZ17-6.02 rapidly activates ATM proteins localized around and outside of the nucleus. Cells were treated with vehicle control or with GZ17-6.02 (2 μ M). Cells were fixed 0.5h and 1h after drug exposure. Cells were fixed in situ, permeabilized, stained with the indicated validated primary antibodies and imaged with secondary antibodies carrying red- and green-fluorescent tags. Total ATM protein levels and ATM localization within the cell did not alter over the time course (data not shown).

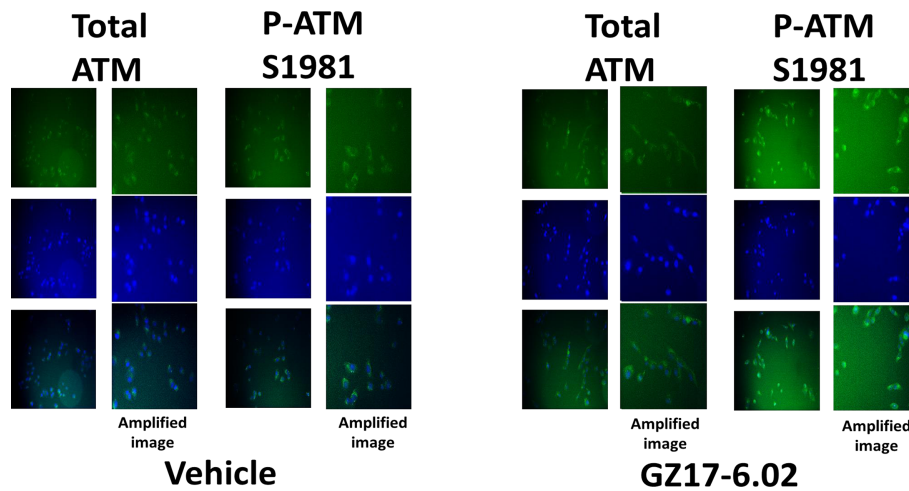


FIGURE 13
 GZ17-6.02 rapidly activates ATM proteins localized around and outside of the nucleus. Cells were treated with vehicle control or with GZ17-6.02 (2 μM). Cells were fixed 6h after drug exposure. Cells were fixed in situ, permeabilized, stained with the indicated validated primary antibodies and imaged with secondary antibodies carrying red- and green-fluorescent tags. Cells were co-stained with DAPI. Total ATM protein levels and ATM localization within the cell did not alter over the time course (data not shown).

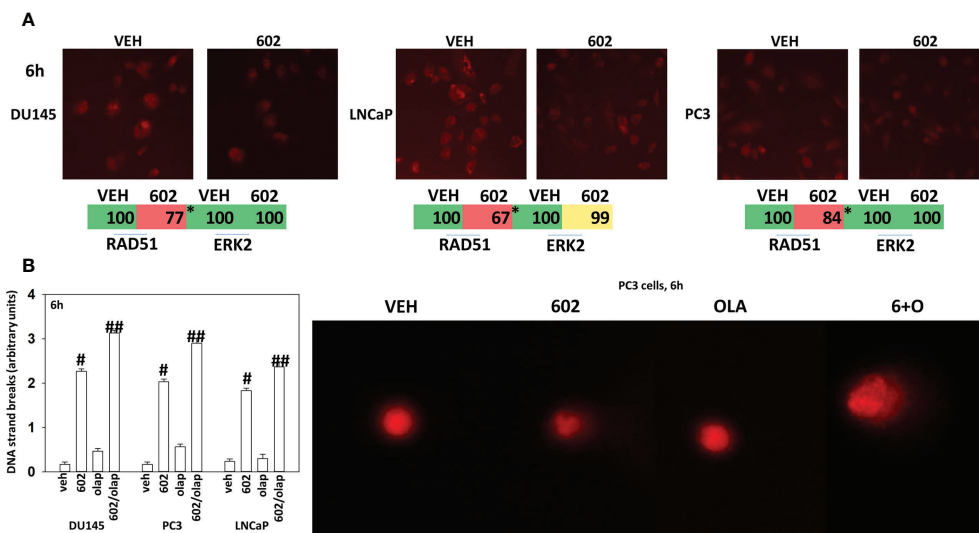


FIGURE 14
 GZ17-6.02 reduces RAD51 expression and increases DNA damage. **(A)** Cells were treated with vehicle control or with GZ17-6.02 (2 μM). Cells were fixed 6h after drug exposure. Cells were fixed in situ, permeabilized, stained with the indicated validated primary antibodies and imaged with secondary antibodies carrying red- and green-fluorescent tags. The staining intensity of at least 100 cells per well/condition is determined in three separate studies. The data are the normalized amount of fluorescence set at 100% comparing intensity values for vehicle control (n = 3 +/-SD). #p < 0.05 greater than vehicle control; *p < 0.05 less than vehicle control. **(B)** Drug-treated cells, in suspension, were mixed with low melting point agarose and spread onto a microscope glass slide. After lysis of cells with detergent at a high salt concentration, DNA unwinding and electrophoresis was carried out at neutral pH (7-8). Tail moments were scored using a Method which classifies comets from grades 0-4 (11-13). One hundred comets were scored, and each comet assigned a value of 0 to 4 according to its class, the mean total score for the sample gel will be between 0 and 4 "arbitrary units." (n = 3 +/-SD) # p < 0.05 greater than vehicle control; ###p < 0.05 greater than GZ17-6.02 alone value.

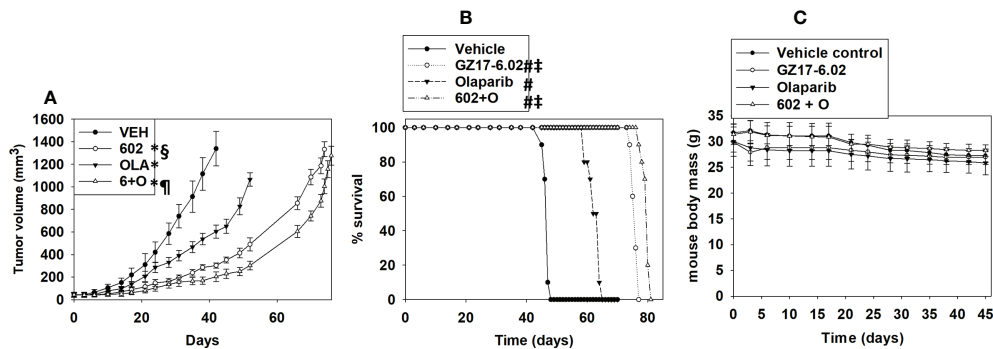


FIGURE 15

GZ17-6.02 profoundly suppresses the growth of AR+ prostate cancer tumors, prolonging survival, and interacts with olaparib to further reduce tumor growth. Male NRG mice supplied by the Massey Cancer Center Animal Core (~20 g) were injected with 1.0×10^6 male LNCaP cells into their rear flank (10 animals per treatment group). Tumors were permitted to form for 1 week with tumors at that time exhibiting a mean volume of approximately 50 mm^3 . Mice were treated by oral gavage once every day for 45 days with vehicle control, GZ17-6.02 (50 mg/kg), olaparib (10 mg/kg) or the drugs in combination. Before, during and after drug treatment tumors were calipered every ~3 days as indicated in (A) and tumor volume was assessed up to 45 days later. Tumor volumes under each condition are plotted. * $p < 0.05$ reduced growth compared to vehicle control; † $p < 0.05$ reduced growth compared to olaparib single agent; ‡ $p < 0.05$ reduced growth compared to GZ17-6.02 single agent. Animals were humanely killed when the tumor volume reached approximately $2,000 \text{ mm}^3$ due to ulceration. Animal survival was plotted on a Kaplan–Meier curve (B). # $p < 0.05$ greater survival than vehicle control; † $p < 0.05$ greater than olaparib single agent. In (C) the body mass of the mice in the study is presented over the 45-day treatment time course.

regrew to such an extent that there was no difference in animal survival. Whether prolonged (> 45 days) exposure of the tumors to GZ17-6.02 and olaparib would ultimately result in a significant enhancement in survival is not known.

Data availability statement

The raw data supporting the conclusions of this article will be made available by the authors, without undue reservation.

Ethics statement

The animal study was reviewed and approved by Studies were performed according to the U.S. Department of Agriculture regulations under the VCU IACUC protocol AD20008.

Author contributions

LB and JR performed the studies. PD directed the studies. CW collaborated with PD to develop the studies and critically read the final manuscript. All authors contributed to the article and approved the submitted version.

Funding

Support for the present study was funded from philanthropic funding from Massey Cancer Center and the Universal Inc. Chair in Signal Transduction Research. PD acknowledges funding Genzada Pharmaceuticals USA, Inc. The funder was not involved in the study design, collection, analysis, interpretation of data, the writing of this article or the decision to submit it for publication.

Acknowledgments

Additional support for the present study was funded from philanthropic funding from Massey Cancer Center and the Universal Inc. Chair in Signal Transduction Research. Services in support of the research project were provided by the VCU Massey Cancer Center Mouse Core, supported, in part, with funding from NIH-NCI Cancer Center Support Grant P30 CA016059. We thank Dr. Roy Sabo (VCU, Biostatistics), for biostatistical assistance during these studies. PD and CW thank Dr. Daniel Von Hoff for expert guidance during performance of these studies and for editing the manuscript.

Conflict of interest

Author CW is a paid officer at Genzada Pharmaceuticals. PD is a Consultant and Key Scientific advisor to Genzada Pharmaceuticals.

The remaining authors declare that the research was conducted in the absence of any commercial or financial relationships that could be construed as a potential conflict of interest.

References

- Booth L, Roberts JL, West C, Von Hoff D, Dent P. GZ17-6.02 initiates DNA damage causing autophagosome-dependent HDAC degradation resulting in enhanced anti-PD1 checkpoint inhibitory antibody efficacy. *J Cell Physiol* (2020) 235:8098–113. doi: 10.1002/jcp.29464
- Booth L, West C, Moore RP, Von Hoff D, Dent P. GZ17-6.02 and pemetrexed interact to kill osimertinib-resistant NSCLC cells that express mutant ERBB1 proteins. *Front Oncol* (2021) 11:711043. doi: 10.3389/fonc.2021.711043
- Booth L, West C, Von Hoff D, Kirkwood JM, Dent P. GZ17-6.02 interacts with [MEK1/2 and b-RAF inhibitors] to kill melanoma cells. *Front Oncol* (2021) 11:656453. doi: 10.3389/fonc.2021.656453
- Booth L, West C, Moore RP, Von Hoff D, Dent P. GZ17-6.02 and palbociclib interact to kill ER+ breast cancer cells. *Oncotarget* (2022) 13:92–104. doi: 10.18632/oncotarget.28177
- West CE, Kwatra SG, Choi J, Von Hoff D, Booth L, Dent P. A novel plant-derived compound is synergistic with 5-fluorouracil and has increased apoptotic activity through autophagy in the treatment of actinic keratoses. *J Dermatolog Treat* (2022) 33:590–1. doi: 10.1080/09546634.2020.1764905
- Dent P, Booth L, Roberts JL, Rais R, Owusu K, Poklepovic A, et al. [Curcumin + sildenafil] enhances the efficacy of 5FU and anti-PD1 therapies in vivo. *J Cell Physiol* (2020) 235:6862–74. doi: 10.1002/jcp.29580
- Mitchell E, Alese OB, Yates C, Rivers B, Blackstock W, Newman L, et al. J Cancer healthcare disparities among African americans in the united states. *Natl Med Assoc* (2022) 114:236–50. doi: 10.1016/j.jnma.2022.01.004
- Fontana F, Anselmi M, Limonta P. Molecular mechanisms and genetic alterations in prostate cancer: From diagnosis to targeted therapy. *Cancer Lett* (2022) 534:215619. doi: 10.1016/j.canlet.2022.215619
- Nigro MC, Mollica V, Marchetti A, Cheng M, Rosellini M, Montironi R, et al. Current androgen receptor antagonists under investigation for resistant prostate cancer. *Expert Rev Anticancer Ther* (2022) 22:191–202. doi: 10.1080/14737140.2022.2020651
- Paulet L, Trecourt A, Leary A, Peron J, Descotes F, Devouassoux-Shisheboran M, et al. Cracking the homologous recombination deficiency code: how to identify responders to PARP inhibitors. *Eur J Cancer*. (2022) 166:87–99. doi: 10.1016/j.ejca.2022.01.037
- Kumaravel TS, Vilhar B, Faux SP, Jha AN. Comet assay measurements: A perspective. *Cell Biol Toxicol* (2009) 25:53–64. doi: 10.1007/s10565-007-9043-9
- Collins AR, Ma AG, Duthie SJ. The kinetics of repair of oxidative DNA damage (strand breaks and oxidised pyrimidine) in human cells. *Mutat Res* (1995) 336:69–77. doi: 10.1016/0921-8777(94)00043-6
- Collins AR. Comet assay for DNA damage and repair: principles, applications and limitations. *Mol Biotechnol* (2004) 26:249–61. doi: 10.1385/MB:26:3:249
- Koromilas AE. Roles of the translation initiation factor eIF2alpha serine 51 phosphorylation in cancer formation and treatment. *Biochim Biophys Acta* (2015) 1849:871–80. doi: 10.1016/j.bbagr.2014.12.007
- Joshi M, Kulkarni A, Pal JK. Small molecule modulators of eukaryotic initiation factor 2 alpha kinases, the key regulators of protein synthesis. *Biochimie* (2013) 95:1980–90. doi: 10.1016/j.biochi.2013.07.030
- Ekaterina Chesnokova E, Bal N, Kolosov P. Kinases of eIF2a switch translation of mRNA subset during neuronal plasticity. *Int J Mol Sci* (2017) 18:2213. doi: 10.3390/ijms18102213
- Kirsch K, Zeke A, Töke O, Sok P, Sethi A, Sebó A, et al. Co-Regulation of the transcription controlling ATF2 phospho-switch by JNK and p38. *Nat Commun* (2020) 11:1–15. doi: 10.1038/s41467-020-19582-3
- Gil J, Alcamí J, Esteban M. Activation of NF- κ B by the dsRNA-dependent protein kinase, PKR involves the I κ B kinase complex. *Oncogene* (2000) 19:1369–78. doi: 10.1038/sj.onc.1203448
- Gil J, Alcamí J, Esteban M. Induction of apoptosis by double-Stranded-RNA-Dependent protein kinase (PKR) involves the α subunit of eukaryotic translation initiation factor 2 and NF- κ B. *Mol Cell Biol* (1999) 19:4653–63. doi: 10.1128/MCB.19.7.4653
- Qiao L, Han SI, Fang Y, Park JS, Gupta S, Gilfor D, et al. Bile acid regulation of C/EBPbeta, CREB, and c-jun function, via the extracellular signal-regulated kinase and c-jun NH2-terminal kinase pathways, modulates the apoptotic response of hepatocytes. *Mol Cell Biol* (2003) 23:3052–66. doi: 10.1128/MCB.23.9.3052-3066.2003
- Jiang J, Jiang B, He Z, Ficarro SB, Che J, Marto JA, et al. Discovery of covalent MKK4/7 dual inhibitor. *Cell Chem Biol* (2020) 27:1553–1560.e8. doi: 10.1016/j.chembiol.2020.08.014
- Kwong AJ, Pham TND, Oelschlager HE, Munshi HG, Scheidt KA. Rational design, optimization, and biological evaluation of novel MEK4 inhibitors against pancreatic adenocarcinoma. *ACS Med Chem Lett* (2021) 12:1559–67. doi: 10.1021/acsmchemlett.1c00376
- Yu-Wei D, Li ZS, Xiong SM, Huang G, Luo YF, Huo TY, et al. Paclitaxel induces apoptosis through the TAK1-JNK activation pathway. *FEBS Open Bio*. (2020) 10:1655–67. doi: 10.1002/2211-5463.12917
- Thomas-Jardin SE, Dahl H, Nawas AF, Bautista M, Delk NA. NF- κ B signaling promotes castration-resistant prostate cancer initiation and progression. *Pharmacol Ther* (2020) 211:107538. doi: 10.1016/j.pharmthera.2020.107538
- Uzzo RG, Crispen PL, Golovine K, Makhov P, Horwitz EM, Kolenko VM. Diverse effects of zinc on NF-kappaB and AP-1 transcription factors: implications for prostate cancer progression. *Carcinogenesis* (2006) 27:1980–90. doi: 10.1093/carcin/bgl034
- Bu Y, Li X, He Y, Huang C, Shen Y, Cao Y, et al. A phosphomimetic mutant of RelA/p65 at Ser536 induces apoptosis and senescence: An implication for tumor-suppressive role of Ser536 phosphorylation. *Int J Cancer* (2016) 138:1186–98. doi: 10.1002/ijc.29852
- Ghosh C, Paul S, Dandawate P, Gunewardena SS, Subramaniam D, West C, et al. Super-enhancers: novel target for pancreatic ductal adenocarcinoma. *Oncotarget* (2019) 10:1554–71. doi: 10.18632/oncotarget.26704
- Itkonen HM, Urbanucci A, Martin SE, Khan A, Mathelier A, Thiede B, et al. High OGT activity is essential for MYC-driven proliferation of prostate cancer cells. *Theranostics* (2019) 9:2183–97. doi: 10.7150/thno.30834
- Baumgart SJ, Nevedomskaya E, Haendler B. Dysregulated transcriptional control in prostate cancer. *Int J Mol Sci* (2019) 20:2883. doi: 10.3390/ijms20122883
- Chen X, Ma Q, Shang Z, Niu Y. Super-enhancer in prostate cancer: transcriptional disorders and therapeutic targets. *NPJ Precis Oncol* (2020) 4:31. doi: 10.1038/s41698-020-00137-0
- Bundred N, Gardovskis J, Jaskiewicz J, Eglitis J, Paramonov V, McCormack P, et al. Evaluation of the pharmacodynamics and pharmacokinetics of the PARP inhibitor olaparib: a phase I multicentre trial in patients scheduled for elective breast cancer surgery. *Invest New Drugs* (2013) 31:949–58. doi: 10.1007/s10637-012-9922-7
- Fong PC, Boss DS, Yap TA, Tutt A, Wu P, Mergui-Roelvink M, et al. Inhibition of poly (ADP-ribose) polymerase in tumors from BRCA mutation carriers. *N Engl J Med* (2009) 361:123–34. doi: 10.1056/NEJMoa0900212

Publisher's note

All claims expressed in this article are solely those of the authors and do not necessarily represent those of their affiliated organizations, or those of the publisher, the editors and the reviewers. Any product that may be evaluated in this article, or claim that may be made by its manufacturer, is not guaranteed or endorsed by the publisher.